applied sciences

MDPI

Article

Fracture Behaviour of Concrete with Reactive Magnesium Oxide as Alternative Binder

J. A. Forero [1], M. Bravo [2], J. Pacheco [3], J. de Brito [3,*] and L. Evangelista [4]

1 Postgraduate Program in Structural Engineering and Construction (PECC), Predio SG-12 Campus Darcy Ribeiro, University of Brasília, Brasilia-DF CEP 70910-900, Brazil; javier.valencia@tecnico.ulisboa.pt
2 CERIS, Escola Superior de Tecnologia do Barreiro, Instituto Politécnico de Setúbal, Rua Américo da Silva Marinho, 2839-001 Lavradio, Portugal; miguelnbravo@tecnico.ulisboa.pt
3 CERIS, Instituto Superior Técnico, Universidade de Lisboa, Av. Rovisco Pais, 1049-001 Lisboa, Portugal; joaonpacheco@tecnico.ulisboa.pt
4 CERIS, Instituto Superior de Engenharia de Lisboa, R. Conselheiro Emídio Navarro, 1950-062 Lisboa, Portugal; evangelista@dec.isel.ipl.pt
* Correspondence: jb@civil.ist.utl.pt

Abstract: This research evaluates the fracture behavior of concrete with reactive magnesium oxide (MgO). Replacing cement with MgO is an attractive option for the concrete industry, mainly due to sustainability benefits and reduction of shrinkage. Four different MgO's from Australia, Canada, and Spain were used in the concrete mixes, as a partial substitute of cement, at 5%, 10%, and 20% (by weight). The fracture toughness (K_I) intensity factor and the stress–strain softening parameters of the wedge split test were evaluated after 28 days. The experimental results showed that the replacement of cement with MgO reduced the fracture energy between 13% and 53%. Moreover, the fracture energy was found to be correlated with both compressive strength and modulus of elasticity. A well-defined relationship between these properties is important for an adequate prediction of the non-linear behavior of reinforced concrete structures made with partial replacement of cement with MgO.

Keywords: reactive magnesium oxide; fracture energy; wedge splitting test; alternative binder; concrete

Citation: Forero, J.A.; Bravo, M.; Pacheco, J.; de Brito, J.; Evangelista, L. Fracture Behaviour of Concrete with Reactive Magnesium Oxide as Alternative Binder. *Appl. Sci.* **2021**, *11*, 2891. https://doi.org/10.3390/app11072891

Academic Editor: Alexey Beskopylny

Received: 22 February 2021
Accepted: 20 March 2021
Published: 24 March 2021

1. Introduction

To reduce the effect of global climate change due to greenhouse gases, many governments around the world have been striving to reduce carbon dioxide's (CO_2) emission rates as the main cause of this effect. One of the sectors with a large share of CO_2 emissions is the construction industry, which is responsible for 10% of the CO_2 expelled to the atmosphere each year [1], with the cement industry alone emitting about 5.7 billion tonnes of CO_2 in 2018 [2]. A path for CO_2 reduction in the construction industry is the use of supplementary cementitious materials, such as fly ash (FA), silica active, slag, metakaolin, reactive MgO, among others. Among these alternatives, reactive MgO has become a good option as a supplementary material, as non-reactive MgO is already used in the composition of cements for refractory use [3]. Yet, standards restrict the content of MgO in clinker to a maximum of 5% [4].

One of the main advantages of using reactive MgO-based cements is that the production of reactive MgO (calcinated at 700 °C to 1000 °C) requires lower temperatures in comparison to the production of clinker (>1400 °C). MgO is mainly produced by calcining mined magnesite deposits ($MgCO_3$). The temperature and calcination time produce changes in the crystalline structure of MgO. For example, with the increase of temperature and calcination time, MgO suffers a reduction in its surface area increasing the size of the crystalline structure and reducing its reactivity [5–7]. The calcination process in obtaining MgO can be identified according to the calcination temperature. The European

Commission has defined the grades of MgO as: caustic calcined (the case of reactive MgO), 600–1300 °C; dead burnt, 1600–2200 °C; and fused, >2800 °C [8].

During mixing, the use of reactive MgO with cement (either in cement production as a small percentage of clinker, or as an addition) results in the formation of $Mg(OH)_2$ (Equation (1)), which subsequently carbonates to a hydrated magnesium carbonate (Equation (2)) [9–11].

$$MgO + H_2O \rightarrow Mg(OH)_2 \quad (1)$$

$$Mg(OH)_2 + CO_2 + 2H_2O \rightarrow MgCO_3.3H_2O \quad (2)$$

MgO can also be used as an expansive additive. This expansive character can be controlled with MgO reactivity and fineness. The higher the MgO calcination temperature, the lower the expansion at early ages, and the longer the hydration process lasts. As the hydration of MgO is a gradual and irreversible process, $Mg(OH)_2$ is stable, and its expansion is stable and not unlimited. The influence on the incorporation of different reactive MgO has shown that, with the use of reactive MgO as binder, there is a reduction of mechanical properties, such as compressive strength [12–22], flexural strength [15,16,19,22–24], and splitting tensile strength [22,25].

More specifically, authors such as Mavroulidou et al. [18] showed that there is a reduction of compressive strength in ternary concrete with fly ash (FA), metakaolin, and reactive MgO. As the MgO ratio is increased, the reduction was about 30%. The water/binder (w/b) ratio was kept constant (0.55) for all the mixes. Mavroulidou et al. [18] attributed this reduction to the fact that MgO increased the porosity and production of magnesium silicate hydrates due to the lack of reaction between FA and Brucite to form the M-S-H gel. In a study by Gao et al. [19], it was observed that the type of curing influences the compressive strength. This property increased by increasing the autoclave time and decreased by increasing the autoclave temperature. The compressive strength values were higher in mixes with 4% MgO, followed by 8% and 12%.

Unluer and Al-Tabbaa [21] studied the compressive strength under conditions of accelerated carbonation (10% of CO_2) in concrete blocks with reactive MgO and FA. The results for compressive strength were about twice those of MgO mixes without FA. This response was attributed to the higher porosity of the FA mixes, leaving more space for the formulation of hydrated magnesium carbonate and strength development. Mixes with higher w/b ratios (0.6 and 0.9) showed poor strength due to low compaction and presence of saturated pores preventing CO_2 and hydrated magnesium carbonate formulation, respectively. The maximum strength was obtained in MgO mixes with w/b ratio of 0.7, with and without FA. The strength of the mixes increased gradually by increasing CO_2 concentration from 0% to 20%. The strength development from one day to seven days decreased by increasing CO_2 concentration.

Tensile strength is also influenced by the use of MgO. Mavroulidou et al. [18] studied the tensile strength of concrete mixes produced with different contents of reactive MgO, FA, and metakaolin. The authors found that the tensile strength slightly decreased (less than 10%) with the use of 10% of MgO and 20% of FA. The modulus of elasticity is also influenced by the incorporation of MgO. Choi et al. [17] studied the modulus of elasticity after freeze–thaw cycles in concrete mixes produced with 20% FA, and different w/b ratios of 0.48 and 0.65, cured with water for 28 days or 360 days. The use of MgO led to a slight influence (4%) of the modulus of elasticity of the concrete mixes after 100, 200, and 300 freeze–thaw cycles.

The existing references show that the use of reactive MgO in concrete leads to higher initial expansion and lower shrinkage [7,26]. However, the MgO incorporation effect is dependent on the MgO reactivity [27] and MgO content [13]. When MgO hydration takes place, the final product is magnesium hydroxide, which has a larger volume than its constituents, decreasing the shrinkage of concrete with MgO [28]. However, concrete made with high reactive MgO may exhibit dimensional stability problems, as the expansive reactions of this material may overcome those due to cement paste shrinkage [29].

The literature does not contain many studies of the fracture properties in concrete with MgO. This property is important to predict structural behavior and to design structural concrete. Wu et al. [30] studied concrete with reactive MgO and fly ash cured with an accelerated carbonating process for one, three, and seven days. The authors observed that the carbonation curing densifies the bonding system, leading to an increase of the retarded tensile strength at first cracking. The changes in volume and microstructure of concrete have great influence on fracture properties of concrete. As a result, the use of an expansive agent like MgO has some influence on the fracture performance of concrete [31]. Guo et al. [31] studied the effects of expansive agents (EA) and MgO on the fracture properties. The results indicated that the trends in the development of concrete fracture parameters varied with curing ages at different proportions of EA, MgO, and FA. Expansive agents generally decrease toughness at initial fracture and toughness against unstable concrete fracture. Guo et al. [31] observed that, when the amount of MgO is increased, the area under the splitting force–crack mouth opening displacement (CMOD) curve becomes relatively large. However, when the amount of MgO is 5%, the curve is relatively flat.

In this study, the influence of the incorporation of MgO at replacement ratios of 5%, 10%, and 20% of cement on the mechanical and fracture behavior of concrete was studied. The relevance of this paper consists in that in the literature there are not enough studies presenting the fracture behavior in concrete with different types of MgO's. This relevance increases with the analysis of three different MgO replacement ratios (5%, 10%, and 20%). Moreover, reactive MgO for concrete is not a commercial product and no standards for its production, properties, and/or specification exist. By analyzing three sources of MgO produced for other industries (e.g., agriculture), the paper analyses whether products readily available in the market suit concrete production. In order to obtain the fracture parameters, compressive strength, tensile strength, and modulus of elasticity tests were carried out, with the intention of having a more comprehensive understanding. In turn, correlations were made between the mechanical properties and fracture properties, to have a complete analysis of the influence of MgO as a partial cement substitute on the fracture behavior. In summary, all the properties analyzed in this paper will serve as a basis to establish the necessary parameters for structural use, missing until now.

2. Materials and Methods

2.1. Experimental Procedure

2.1.1. Materials

The cement used as the main binder for the mix composition reference concrete (RC) was CEM I 42.5 R produced by Secil (Lisboa, Portugal). In this study, two types of natural aggregates were used: coarse aggregates (with commercial grading conforming with the designations 2/6, 6/12 and 12/20 of EN 12620 [32]); siliceous sands (0/2 and 0/4). These products are marked for EN 12620 [32].

The reactive MgO's used in this research were manufactured in three different countries (Australia, Canada, and Spain), and were defined as A, C, and S0, respectively. To analyze the influence of particle size, a grinding treatment was carried out on the MgO from Spain for one hour in a rotary mill with steel balls of diameter 2–4 cm to obtain a particle size distribution comparable to that of cement and named S1. Regarding the MgO's from Australia and Canada, no treatment was performed because their particle size was already similar to that of cement. In summary, the influence of four types of MgO's as partial replacement of cement was analyzed.

Table 1 shows the results obtained in the tests to determine the specific surface, purity, reactivity, and skeletal density of the various MgO analyzed. Specific surface affects the reactivity of MgO and is therefore an extremely important factor. In turn, the purity of MgO makes it possible to determine how many other elements there are in the different MgO's received from the manufacturers. This factor also significantly influences the behavior of concrete produced with these materials.

Table 1. Characteristics of the various reactive MgO's and cement.

	MgO-S0	MgO-S1	MgO-C	MgO-A	Cement
Purity (%)	85.0	86.3	96.0	98.8	-
Specific surface (m^2/g)	4.9	3.0	47.9	51.2	2.8
Reactivity (s)	3544	1460	16	14	-
Skeletal density (kg/m^3)	3071	3111	3371	3584	3110

From Table 1, it can be concluded that MgO-C, and MgO-A have reactivities and specific surfaces much higher than those of cement and other MgO's. Liska et al. [33] also showed that the reactivity of MgO increases by reducing its particle size and, consequently, increasing its specific surface area. It can also be seen that the product from Australia has the highest content of MgO in its constitution (98.8%). All MgO's have a purity higher than 85%.

2.1.2. Mix Design

The mixes' composition was based on the methodology proposed by Nepomuceno et al. [34], taking into account the following parameters: C30/37 strength class, XC3 exposure class, and S2 slump in accordance with the EN 206 standard [35]. The materials' contents of the mixes, in volume, are provided in Table 2. All the mixes were designed based on the same composition, with different w/c ratios required to keep all mixes within the target slump.

Table 2. Composition of the mixes (kg/m^3).

Mixes Name	Quantity of Water	Quantity of Cement	Quantity of MgO	Quantity of Fine Aggregates	Quantity of Coarse Aggregates	Fresh-State Density
RC	174	300	0	883	997	2427.5
C5:C	179	285	15	883	997	2455.0
C10:C	182	270	30	883	997	2372.8
C20:C	188	240	60	883	997	2363.1
C5:S0	175	285	15	883	997	2452.0
C10:S0	175	270	30	883	997	2463.7
C20:S0	176	240	60	883	997	2442.0
C5:S1	175	285	15	883	997	2440.8
C10:S1	175	270	30	883	997	2457.6
C20:S1	176	240	60	883	997	2465.0
C5:A	178	285	15	883	997	2403.5
C10:A	182	270	30	883	997	2401.6
C20:A	182	240	60	883	997	2397.1

Concrete production was done in three phases with a total mixing time of 10 min. The first phase lasted 4 min and the coarse aggregates were mixed with 2/3 of the total mixing water. In the second phase, the fine aggregates were added and mixing lasted two minutes. The third phase consisted of adding the cement with the remaining 1/3 of the water in the mix for four minutes. The replacement of cement with reactive MgO was made by mass at 5%, 10%, and 20%. These percentages were defined according to the results obtained in a previous investigation [22]. There, the mechanical and durability behavior of mortars with reactive MgO was studied, using replacement ratios of 0%, 5%, 10%, 15%, 20%, and 25% by mass. The mixes were named as follows: RC for the reference concrete without any reactive MgO, concrete with partial replacement of reactive MgO from Spain and without grinding treatment was named S0, concrete with reactive MgO and with one-hour grinding treatment was named S1, and concrete with MgO's from Australia and Canada was named A and C, respectively. To designate the MgO incorporation ratio in the mixes, the nomenclature that designates first the amount of substitution and then the origin, was used, e.g., C5:C describes a concrete with 5% MgO from Canada.

Table 2 also shows the results of the fresh-state density of concrete. It shows that the density remains constant as the MgO incorporation ratio increases.

By increasing the incorporation ratio of reactive MgO, the consistency of the mixes tended to decrease. Therefore, it was necessary to increase the water/binder ratio in the mixes as reactive MgO increased to maintain the target consistency, as observed in Figure 1a. Figure 1b shows that all mixes are within the S2 consistency range as the content of reactive MgO increases.

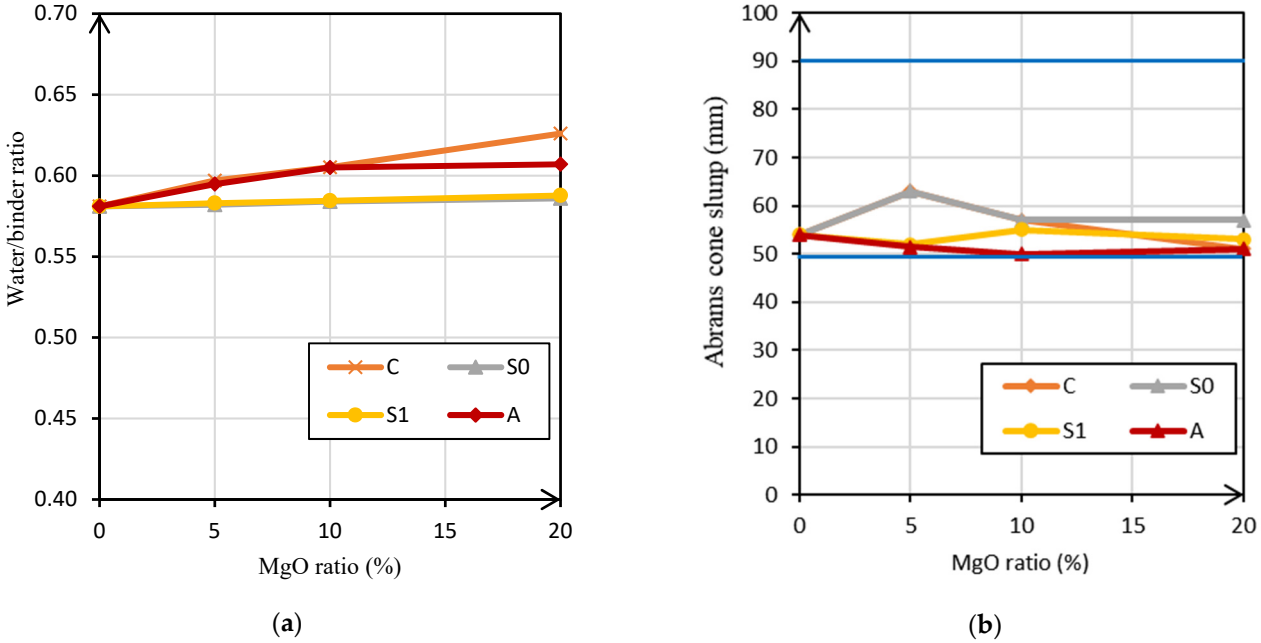

Figure 1. Water/binder ratio of each mix concrete (**a**); Abrams cone consistency according to the MgO content (**b**).

2.1.3. Tests

Fracture energy is the quantity of energy required for the propagation of crack through a unitary area. This property is strongly related to the tensile behaviour of the material. Thus, to better analyze the results obtained in the fracture energy test, other mechanical properties of concrete were analyzed (compressive strength, splitting tensile strength, and modulus of elasticity) after 28 days of curing in a wet chamber. The compressive strength of hardened specimens was evaluated according to EN 12390-3 [36]. This test was performed on four specimens of 150 × 150 × 150 mm. The splitting tensile strength test followed the method presented in EN 12390-6 [37]. This test was performed on three cylindrical specimens of 150 mm diameter × 300 mm high. The test procedure used to determine the secant modulus of elasticity is described in LNEC E 397 [38]. This test was performed on two cylindrical specimens of 150 mm diameter × 300 mm high.

The fracture energy (G_F) was determined using the wedge splitting test (WST) [39], following the procedure described in NT BUILD 511 [40]. WST was performed on four cubic samples of 150 × 150 × 150 mm tested after 28 days of curing in a wet chamber. G_F is determined as the average area under the curve of the splitting force–crack mouth opening displacement (CMOD). This method minimizes the effect of weight on the fracture energy, in contrast to other methods [39–42]. The geometric configuration of the specimens was generated using special moulds in the casting, the guides and the starting notches were made after 15 days of wet curing using a 1 mm diamond saw as shown in Figure 2a,b. The test procedure applies a vertical force (F_v) at a deformation speed of 0.006 mm/sec that divides the test specimen into two sections. During the test, CMOD was continuously measured with a clip gauge as F_v increased. After the test, the depth and width of the split surface (A_{lig}) were measured.

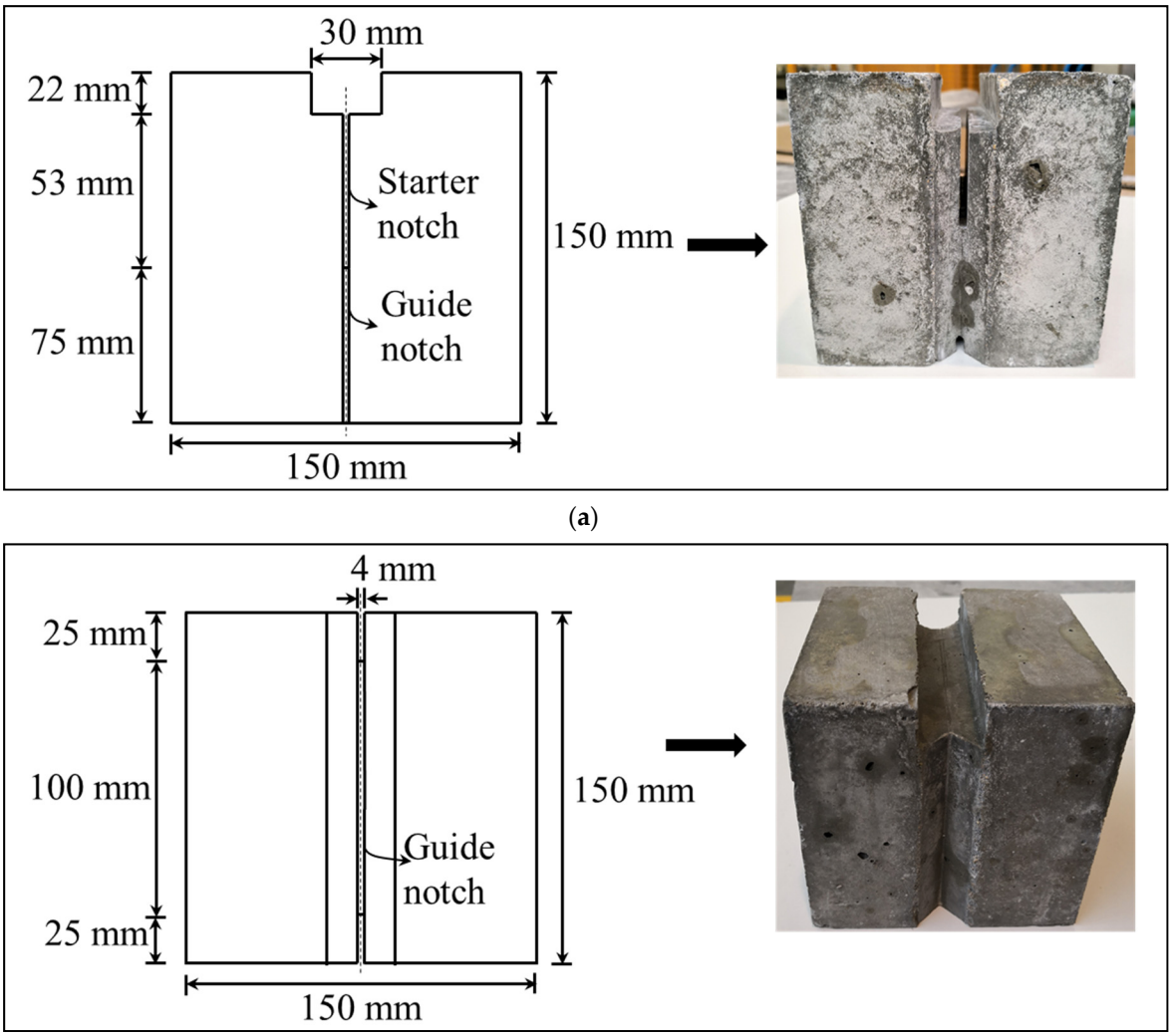

Figure 2. Illustration of the specimens' geometry: front view (**a**); top view (**b**).

The preparation steps to perform WST are illustrated in Figure 3. The splitting force (F_{sp}) was determined from WST using Equation (3), where α is the angle between the wedge and the vertical load line. The area of the splitting force–COMD curve is the energy dissipated during the fracture, $W_{f,CMOD}$, and is normalized with respect to the total split surface (A_{lig}) to complement the fracture. This intermediate specific fracture energy is denoted G_F (kN/mm) and is determined from the test result through Equation (4) [39,40,42].

The double K fracture and the double G_F fracture criteria are based on asymptotic linear superposition, maintaining the relationship of the linear elastic fracture mechanics valid at all points of the splitting force–CMOD envelope. Therefore, the effective double K_I fracture is obtained in terms of equivalent stress intensity factors using the double G_F fracture model. Equation (5) relates the two criteria: double K_I fracture model and double G_F fracture model [43].

$$F_{sp} = \frac{F_V}{2\tan(\alpha)} \quad (3)$$

$$G_F = \frac{W_{f,CMOD}}{A_{lig}} \quad (4)$$

$$K_I = (G_F E_{cm})^{\frac{1}{2}} \quad (5)$$

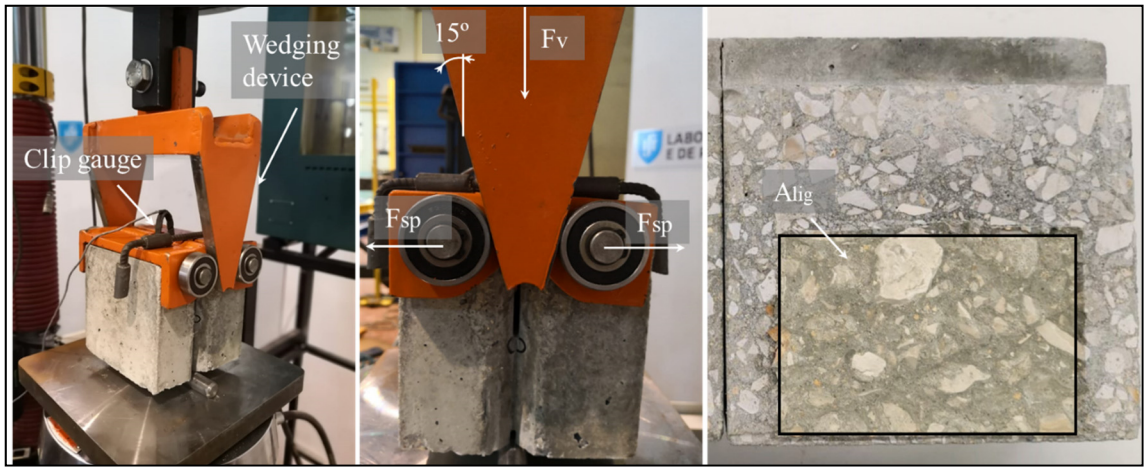

Figure 3. Illustration of the application of the splitting load.

3. Experimental Results and Discussion

3.1. Main Mechanical Properties

Table 3 shows the results of the compressive strength, splitting tensile strength, and modulus of elasticity tests, as well as their standard deviations and the percentage of variation with respect to RC.

Table 3. Main mechanical properties.

Mix	Compressive Strength			Tensile Strength			Modulus of Elasticity		
	28	σ	Δ_{RC}	28	σ	Δ_{RC}	28	σ	Δ_{RC}
RC	51.05	1.70	-	3.58	0.16	-	36.57	0.02	-
C5:C	46.17	1.36	−9.6%	3.20	0.24	−10.5%	42.07	0.20	15.0%
C10:C	40.07	1.12	−21.5%	2.57	0.19	−28.2%	39.03	0.59	6.7%
C20:C	33.60	0.70	−34.2%	2.29	0.03	−36.0%	37.00	1.45	1.2%
C5:S0	40.83	1.27	−20.0%	3.28	0.11	−8.3%	42.40	0.68	15.9%
C10:S0	40.74	0.01	−20.2%	2.92	0.12	−18.5%	39.79	0.72	8.8%
C20:S0	40.11	1.04	−21.4%	2.45	0.39	−31.5%	37.62	0.03	2.9%
C5:S1	44.59	2.40	−12.7%	2.96	0.10	−17.2%	41.73	0.32	14.1%
C10:S1	43.70	2.40	−14.4%	2.80	0.05	−21.9%	40.38	0.38	10.4%
C20:S1	38.32	0.54	−24.9%	2.31	0.19	−35.6%	39.61	0.50	8.3%
C5:A	46.54	3.69	−8.8%	3.50	0.20	−2.2%	41.58	0.15	13.7%
C10:A	43.43	0.25	−14.9%	3.20	0.04	−10.5%	39.37	0.00	7.7%
C20:A	38.46	1.56	−24.7%	2.38	0.16	−33.6%	34.44	0.90	−5.8%

The compressive strength was determined after 28 days of curing in a wet chamber. It is found show that, with the increase of the reactive MgO incorporation ratio, there is a reduction in compressive strength. The effect of the use of MgO can be due to the fact that, firstly, as MgO increases, the amounts of C2S and C3S decrease. Thus, there is a reduction of the formation of C-S-H phases, increasing the formation of $Mg(OH)_2$, which is a less resistant hydration product [16,44,45]. The second reason for these findings concerns the expansive nature of MgO. Reactive MgO can cause cracking and thus lead to an increase in porosity and macro-pores, which is a determining factor in strength [12,46]. The concrete mixes most affected by the incorporation of MgO were those made with C, with a reduction of 33.6% for a ratio of 20% of MgO. This negative influence of these MgO's may be because these mixes needed an increase of water/binder ratio. On the contrary, the less affected mixes were those produced with A. In these cases, the use of 20% of these MgO's caused maximum reductions of 24.7%. Regarding the use of 5% MgO, all mixes showed a decrease of between 8.8% and 20%. Similar behavior was found by

Choi et al. [17], who observed reductions of between 5% and 13% for curing ages of 7 and 28 days in mixes with incorporation of 5% MgO and 20% FA.

The results of the tensile strength test performed after 28 days show that, for the mixes with incorporation ratio of 5% MgO, the reduction was between 2% and 17%. The C5-S0 and C5-A mixes are the ones that had the best behavior with the use of 5% MgO. This can be possibly explained because these mixes have a w/b ratio equal or slightly higher than the w/b ratio of the RC mix. The mixes with MgO S1 had the worst results, with reductions of 17.2%, 21.9%, and 35.6%, for ratios of 5%, 10%, and 20%, respectively. This behavior is because the grinding of MgO from Spain decreased the surface area of the particle, not completely hydrating the MgO particles. Mavroulidou et al. [18] found reductions in tensile strength when 10% reactive MgO was added to the fuel ash and metakaolin binary mixes.

There is an increase in modulus of elasticity when MgO's C, SO and S1 are used at almost all ratios of substitution. These increases are up to 16%, presenting better results for MgO S1 mixes, with values between 8% and 14%. Mixes with MgO A had an improvement at 5% and 10% MgO ratios, with values of 14% and 8%, respectively, and a reduction of 6% for 20% MgO. This increase can be explained by the expansive nature of MgO, decreasing the shrinkage and the micro-cracks and increasing the bulk density of concrete [28,47,48].

Figure 4a shows the relationship between compressive strength and splitting tensile strength in cylindrical specimens for all mixes at 28 days. All mixes were found to be well within the confidence intervals for compressive strength of conventional concrete.

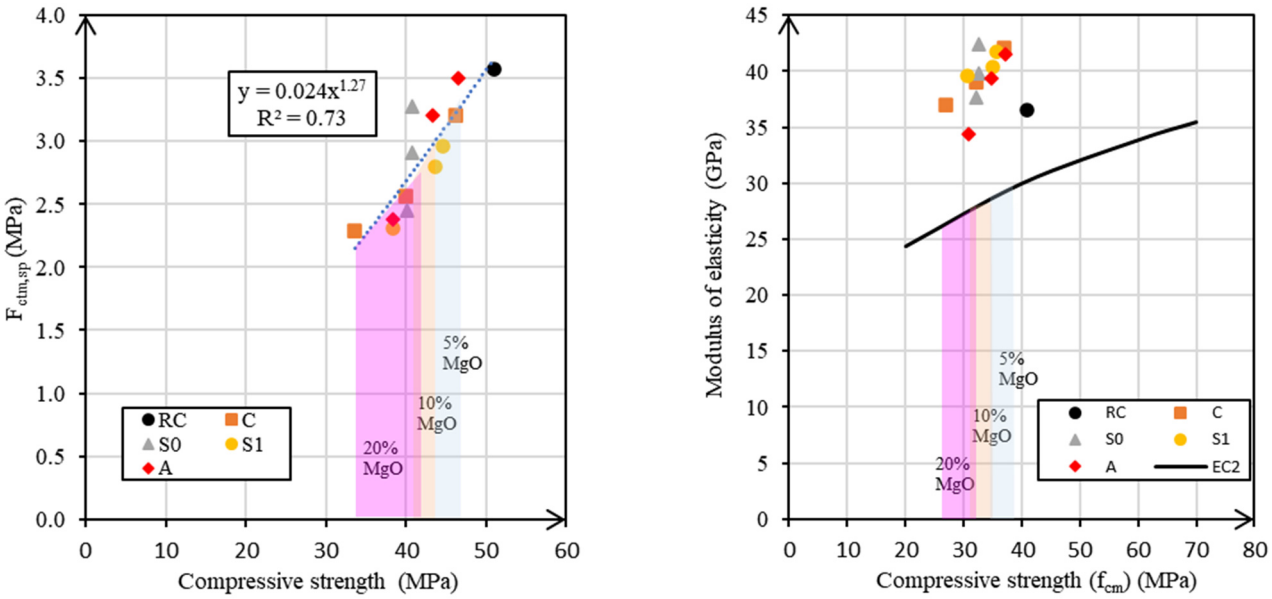

(**a**) (**b**)

Figure 4. Relationship between compressive strength and cylindrical specimens ($f_{cm,sp}$) at 28 days (**a**); relationship between modulus of elasticity and compressive strength (f_{cm}) at 28 days (**b**).

Figure 4b shows the theoretical relationship between the compressive strength and the modulus of elasticity of concrete, according to Equation (6) proposed by EC2 [49], where $\alpha = 0.9$ for coarse limestone aggregates (the case of this paper). It can be observed that all mixes have values of modulus of elasticity much higher than those proposed by EC2. Thus, it is concluded that the proposal established by EC2 [49] is quite conservative.

$$E_{cm} = \alpha\, 22 \left(\frac{f_{cm}}{10}\right)^{0.3} \quad (6)$$

3.2. Fracture Energy

The results of the fracture energy after 28 days of curing are shown in Figure 5a–d and Table 4, as well as their standard deviation and percent variation relative to RC for each substitution ratio. As can be seen there, the fracture energy decreases with the use of reactive MgO. This can be explained because G_F is directly related to the interaction between cement matrix and aggregates. Therefore, the greater the replacement of cement with MgO, the lower the amount of CSH produced and the greater the amount of $Mg(OH)_2$ produced, reducing the properties of the cementitious paste (as inferred from the results of Table 3) and, consequently, the G_F of the concrete mixes [9,10,50,51]. The mixes with MgO from Canada and Australia are the most affected, with a reduction of approximately 50%, relative to RC, for ratio of 20%. In addition to being related to the hydration products formed by the MgO, these mixes have a higher w/b ratio and K_F decreases with the increase of this ratio, as observed by Wittmann and Sadhana [50].

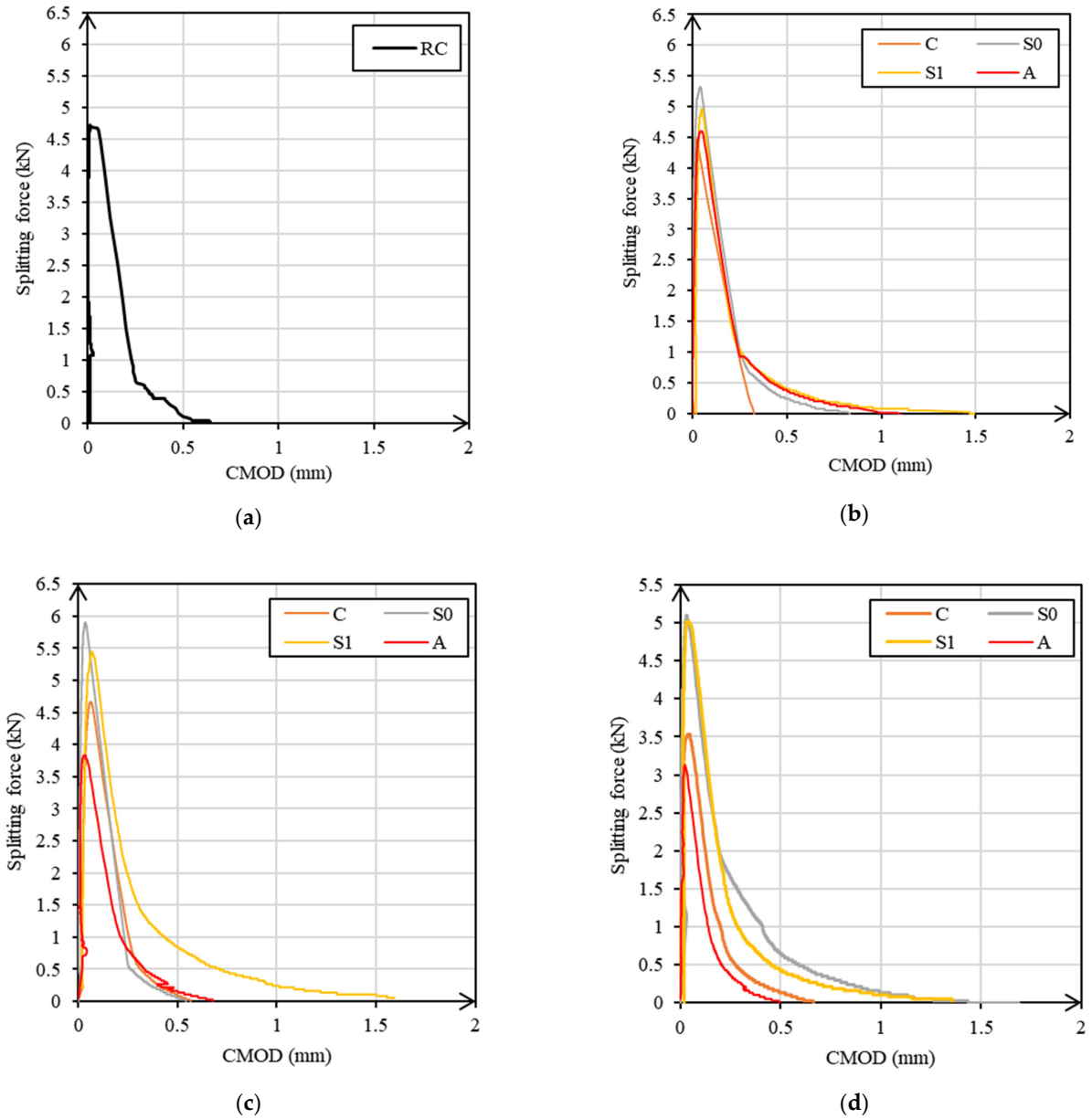

Figure 5. Splitting force versus crack mouth opening displacement (CMOD) curves for mixes: C, S0, S1, A, and RC (**a**), 5% (**b**), 10% (**c**), 20% of MgO (**d**).

Table 4. Fracture energy (G_F) and fracture toughness (K_I) results at 28 days.

Mix	28 Days					
	G_F (N/m)	σ	Δ_{RC}	K_I (MPa·m$^{1/2}$)	σ	Δ_{RC}
RC	141.1	10.3	-	2.27	0.08	-
C5:C	120.7	19.6	−14%	2.25	0.18	−1%
C10:C	117.3	19.6	−17%	2.13	0.17	−6%
C20:C	70.9	11.2	−50%	1.61	0.13	−28%
C5:S0	123.4	0.0	−13%	2.28	0.00	−1%
C10:S0	122.0	4.1	−13%	2.20	0.04	−2%
C20:S0	119.3	0.7	−15%	2.11	0.01	−6%
C5:S1	122.3	0.0	−13%	2.25	0.00	−1%
C10:S1	121.1	14.7	−14%	2.21	0.14	−2%
C20:S1	113.0	14.3	−20%	2.11	0.14	−7%
C5:A	100.0	17.9	−29%	2.03	0.18	−10%
C10:A	95.1	14.2	−33%	1.93	0.16	−15%
C20:A	66.4	10.3	−53%	1.51	0.11	−33%

Figure 5b shows that the tenacity of the mixes with MgO from Australia (A) at 5% (Figure 5b), 10% (Figure 5c), and 20% (Figure 5d) of substitution is lower than that of the mixes with other MgO's. The best results are observed in the mixes with MgO's S0 and S1, as shown in Figure 5b–d. As seen in Figure 5a–d, when the amount of MgO increases, the splitting force–CMOD curve tends to be flatter. Furthermore, CMOD increases with the incorporation of MgO. This increase occurs because the modulus of elasticity of concrete increases with the use of the expansive agent (MgO), improving the quality of concrete [31,48], as was observed in the analysis of results of the modulus of elasticity.

The peak splitting force will also increase for the mixes with MgO S0 and S1, in relation to the RC mix. A similar behavior was observed by Guo et al. [31], when they studied the effect of expansive agents, including MgO, in concrete with FA. The authors observed that toughness exceeded 1.1 times that of the reference concrete between 28 and 60 days using this type of agents.

As G_F and K_I are correlated parameters. In Figure 6a it is found that there is a real logarithmic correlation between these parameters with an R^2 of 0.96. On the other hand, G_F and the compressive strength of each type of concrete mixes are also correlated with a strong quadratic fit (R^2 between 0.93 and 0.99), as shown in Figure 6b. This occurs because one of the most relevant parameters that determine the fracture energy of normal strength concrete is the w/b ratio [52], as is also the case of compressive strength. However, some other properties can also affect the value of G_F, such as the relative strength between aggregates and cement paste [52].

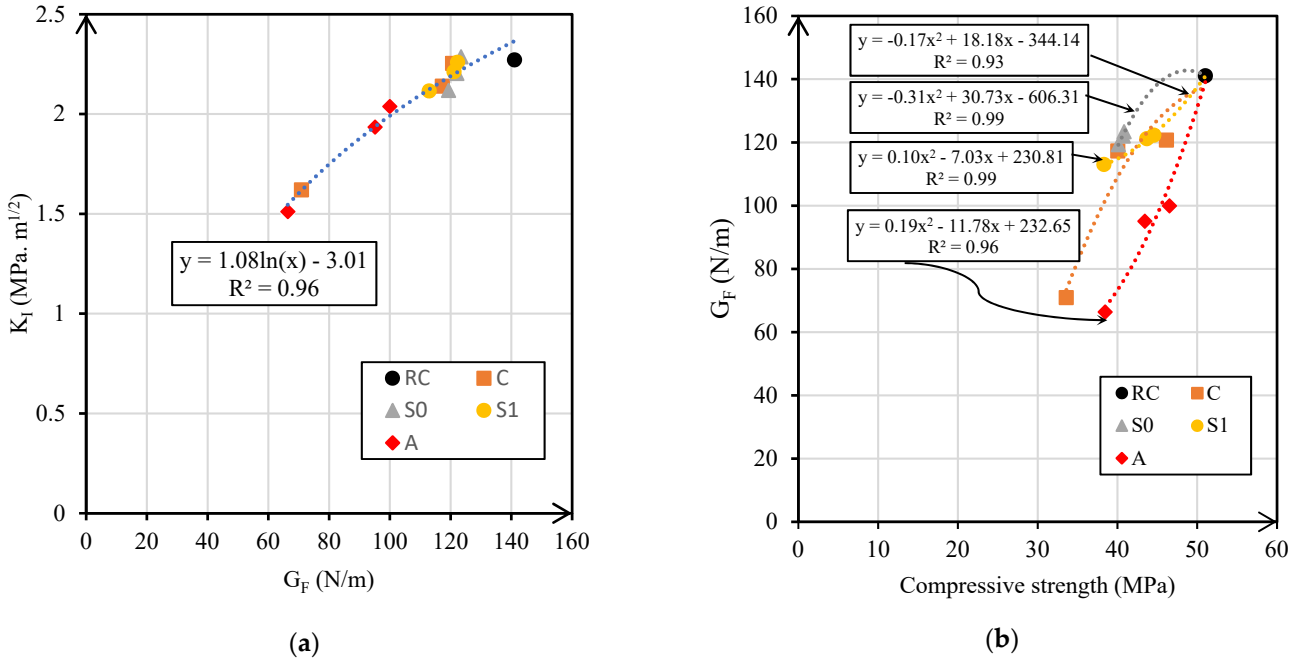

Figure 6. Relationship between fracture energy (G_F) versus strength and fracture toughness (K_I) (**a**) and compressive strength versus fracture energy (G_F) (**b**).

4. Conclusions

From the analysis of the main mechanical properties and of the fracture energy of concrete mixes with partial replacement of cement with reactive MgO, some conclusions were obtained.

The incorporation of MgO usually reflects negatively on the mechanical properties. This is due to the fact that the formation of the hydration product $Mg(OH)_2$ increases and, consequently, there is a weakness of the interfacial transition zone (ITZ), mainly responsible for the mechanical response. The greatest reductions were found in mixes with MgO from Canada (MgO-C), with a maximum reduction of 36% of the splitting tensile strength. As previously explained, this was because this mix contains a higher w/b ratio, generating greater porosity. Regarding the treatment of MgO from Spain, it was possible to conclude that the mixes with MgO S1 had the worst results. This behavior is because the grinding of MgO from Spain decreased the surface area of the particle, not allowing complete hydration of the MgO particles. The modulus of elasticity did not decrease with the use of reactive MgO. In some mixes, there were improvements of up to 15%. This increase can be explained by the expansive nature of reactive MgO. This characteristic of MgO leads to a decrease of shrinkage and micro-cracks and, consequently, to an increase of the modulus of elasticity.

Regarding G_F, it is possible to conclude that toughness is reduced to 53% for the greatest replacement of MgO (20%). However, the splitting force–CMOD response has a softened behavior because MgO is an expansive agent reducing micro-cracks. The best results were observed for MgO's from Spain, with a reduction between 15% and 20% (for 20% MgO). For substitutions between 5% and 10%, all mixes presented similar values of 13–20%, except the one with MgO from Australia, which had major reductions. K_I, being related to G_F and the modulus of elasticity, showed the same trend, with a good correlation with these two properties (R^2 of 0.96). Finally, with these results, it was possible to establish the necessary parameters to characterize a useful stress–strain curve for structural design and numerical modeling.

Author Contributions: Conceptualization, M.B., J.d.B., L.E. and J.P.; Methodology, M.B., J.d.B., L.E. and J.P.; Formal analysis, J.A.F., M.B., J.d.B. and L.E.; Data curation, J.A.F., M.B., J.d.B. and L.E.; Writing—original draft, J.A.F.; Writing—review and editing, M.B., J.P., J.d.B. and L.E. All authors have read and agreed to the published version of the manuscript.

Funding: The authors wish to thank CERIS (Civil Engineering Research and Innovation for Sustainability) research centre and FCT (Foundation for Science and Technology).

Institutional Review Board Statement: Not applicable.

Informed Consent Statement: Not applicable.

Data Availability Statement: No new data were created or analyzed in this study. Data sharing is not applicable to this article.

Conflicts of Interest: The authors declare no conflict of interest.

References

1. Unite Nations Environment Programme. *2020 Global Status Report for Building and Construction: Towards a Zero-emission, Efficient and Resilient Buildings and Construction Sector*; Unite Nations Environment Programme: Nairobi, Kenya, 2020.
2. Andrew, R.M. Global CO_2 emissions from cement production. *Earth Syst. Sci. Data* **2018**, *10*, 195. [CrossRef]
3. Amaral, L.; Oliveira, I.; Salomão, R.; Frollini, E.; Pandolfelli, V. Temperature and common-ion effect on magnesium oxide (MgO) hydration. *Ceram. Int.* **2010**, *36*, 1047–1054. [CrossRef]
4. EN 197-1:2011. *Cement—Part 1: Composition, Specifications and Conformity Criteria for Common Cement*; European Committee for Standardization (CEN): Brussels, Belgium, 2011.
5. Canterford, J. Magnesia—An important industrial mineral: A review of processing options and uses. *Miner. Procesing Extr. Metall. Rev.* **1985**, *2*, 57–104. [CrossRef]
6. Green, J. Calcination of precipitated Mg $(OH)_2$ to active MgO in the production of refractory and chemical grade MgO. *J. Mater. Sci.* **1983**, *18*, 637–651. [CrossRef]
7. José, N.; Ahmed, H.; Miguel, B.; Luís, E.; Jorge, d.B. Magnesia (MgO) Production and Characterization, and Its Influence on the Performance of Cementitious Materials: A Review. *Materials* **2020**, *13*, 4752. [CrossRef]
8. Schorcht, F.; Kourti, I.; Scalet, B.M.; Roudier, S.; Sancho, L.D. *Best Available Techniques (BAT) Reference Document for the Production of Cement, Lime and Magnesium Oxide*; European Commission Joint Research Centre Institute for Prospective Technological Studies: Luxembourg, 2013.
9. Mo, L.; Deng, M.; Tang, M.; Al-Tabbaa, A. MgO expansive cement and concrete in China: Past, present and future. *Cem. Concr. Res.* **2014**, *57*, 1–12. [CrossRef]
10. Zhang, S.; Lee, W. *Spinel-Containing Refractories*; The University of Sheffield: Sheffield, UK, 2004; Volume 178, p. 215.
11. Walling, S.A.; Provis, J.L. Magnesia-based cements: A journey of 150 years, and cements for the future? *Chem. Rev.* **2016**, *116*, 4170–4204. [CrossRef]
12. Zheng, L.; Xuehua, C.; Mingshu, T. MgO-type delayed expansive cement. *Cem. Concr. Res* **1991**, *21*, 1049–1057. [CrossRef]
13. Abdalqader, A.; Al-Tabbaa, A. Mechanical and Microstructural Characterisation of Multicomponent Blended Cements Incorporating Reactive Magnesia. In Proceedings of the 1st Concrete Innovation Cnference (CIC), Oslo, Norway, 11–13 June 2014; The Norwegian Concrete Association–Norsk Betongforening: Oslo, Norway, 2014.
14. Mo, L.; Zhang, F.; Deng, M. Effects of carbonation treatment on the properties of hydrated fly ash-MgO-Portland cement blends. *Constr. Build. Mater.* **2015**, *96*, 147–154. [CrossRef]
15. Mo, L.; Liu, M.; Al-Tabbaa, A.; Deng, M.; Lau, W.Y. Deformation and mechanical properties of quaternary blended cements containing ground granulated blast furnace slag, fly ash and magnesia. *Cem. Concr. Res* **2015**, *71*, 7–13. [CrossRef]
16. Mo, L.; Liu, M.; Al-Tabbaa, A.; Deng, M. Deformation and mechanical properties of the expansive cements produced by inter-grinding cement clinker and MgOs with various reactivities. *Constr. Build. Mater.* **2015**, *80*, 1–8. [CrossRef]
17. Choi, S.-w.; Jang, B.-s.; Kim, J.-h.; Lee, K.-m. Durability characteristics of fly ash concrete containing lightly-burnt MgO. *Constr. Build. Mater.* **2014**, *58*, 77–84. [CrossRef]
18. Mavroulidou, M.; Morrison, T.; Unsworth, C.; Gunn, M. Properties of concrete made of multicomponent mixes of low-energy demanding binders. *Constr. Build. Mater.* **2015**, *101*, 1122–1141. [CrossRef]
19. Gao, P.-w.; Wu, S.-x.; Lu, X.-l.; Deng, M.; Lin, P.-h.; Wu, Z.-r.; Tang, M.-s. Soundness evaluation of concrete with MgO. *Constr. Build. Mater.* **2007**, *21*, 132–138. [CrossRef]
20. Cao, F.; Yan, P. The influence of the hydration procedure of MgO expansive agent on the expansive behavior of shrinkage-compensating mortar. *Constr. Build. Mater.* **2019**, *202*, 162–168. [CrossRef]
21. Unluer, C.; Al-Tabbaa, A. Impact of hydrated magnesium carbonate additives on the carbonation of reactive MgO cements. *Cem. Concr. Res.* **2013**, *54*, 87–97. [CrossRef]
22. Bravo, M.; Forero, J.A.; Nobre, J.; de Brito, J.; Evangelista, L. Performance of Mortars with Commercially-Available Reactive Magnesium Oxide as Alternative Binder. *Materials* **2021**, *14*, 938. [CrossRef]

23. Moradpour, R.; Taheri-Nassaj, E.; Parhizkar, T.; Ghodsian, M. The effects of nanoscale expansive agents on the mechanical properties of non-shrink cement-based composites: The influence of nano-MgO addition. *Compos. Part B Eng.* **2013**, *55*, 193–202. [CrossRef]
24. Lau, W.Y. *The Role of Reactive MgO as an Expansive Additive in the Shrinkage Reduction of Concrete*; University of Cambridge: Cambridge, UK, 2019.
25. Pu, L.; Unluer, C. Investigation of carbonation depth and its influence on the performance and microstructure of MgO cement and PC mixes. *Constr. Build. Mater.* **2016**, *120*, 349–363. [CrossRef]
26. Gonçalves, T.; Silva, R.; De Brito, J.; Fernández, J.; Esquinas, A. Hydration of reactive MgO as partial cement replacement and its influence on the macroperformance of cementitious mortars. *Adv. Mater. Sci. Eng.* **2019**, 1–12. [CrossRef]
27. Wogelius, R.A.; Refson, K.; Fraser, D.G.; Grime, G.W.; Goff, J.P. Periclase surface hydroxylation during dissolution. *Geochim. Et Cosmochim. Acta* **1995**, *59*, 1875–1881. [CrossRef]
28. Du, C. A review of magnesium oxide in concrete. *Concr. Int.* **2005**, *27*, 45–50.
29. Rehsi, S. Magnesium oxide in portland cement. In *Advances in Cement Technology*; Elsevier: Amsterdam, The Netherlands, 1983; pp. 467–483.
30. Wu, H.-L.; Zhang, D.; Ellis, B.R.; Li, V.C. Development of reactive MgO-based Engineered Cementitious Composite (ECC) through accelerated carbonation curing. *Constr. Build. Mater.* **2018**, *191*, 23–31. [CrossRef]
31. Guo, J.; Zhang, S.; Guo, T.; Zhang, P. Effects of UEA and MgO expansive agents on fracture properties of concrete. *Constr. Build. Mater.* **2020**, *263*, 120245. [CrossRef]
32. *EN 12620:2002+A1:2010, Aggregates for Concrete*; European Committee for Standardization (CEN): Brussels, Belgium, 2010.
33. Hewlett, P.; Liska, M. *Lea's Chemistry of Cement and Concrete*; Butterworth-Heinemann: Oxford, UK, 2019.
34. Nepomuceno, M.; Oliveira, L.; Lopes, S.M.R. Methodology for mix design of the mortar phase of self-compacting concrete using different mineral additions in binary blends of powders. *Constr. Build. Mater.* **2012**, *26*, 317–326. [CrossRef]
35. *EN 206:2013+A1:2016 Concrete-Specification, Performance, Production and Conformity*; European Committee for Standardization (CEN): Brussels, Belgium, 2016.
36. EN 12390: 2009. *Testing Hardened Concrete-Part 3: Compressive Strength of Test Specimens*; European Committee for Standardization (CEN): Brussels, Belgium, 2009.
37. EN 12390-6: 2009. *Testing Hardened Concrete Part 6: Tensile Splitting Strength of Test Specimens*; British Standard Institute: Londin, UK, 2009.
38. LNEC. *397, "Betões: Determinação do Módulo de Elasticidade em Compressão"*; LNEC Lisboa: Lisboa, Portugal, 1993.
39. Brühwiler, E.; Wittmann, F. The wedge splitting test, a new method of performing stable fracture mechanics tests. *Eng. Fract. Mech.* **1990**, *35*, 117–125. [CrossRef]
40. BUILD, N. *511: Wedge Splitting Test Method (WST)–Fracture Testing of Fibre-Reinforced Concrete (Mode I)*; Nordic Innovation Centre: Oslo, Norway, 2005; pp. 1–6.
41. Linsbauer, H.; Tschegg, E. Fracture energy determination of concrete with cube-shaped specimens. *Zem. Und Beton* **1986**, *31*, 38–40.
42. Khalilpour, S.; BaniAsad, E.; Dehestani, M. A review on concrete fracture energy and effective parameters. *Cem. Concr. Res.* **2019**, *120*, 294–321. [CrossRef]
43. Kumar, S.; Barai, S.V. *Concrete Fracture Models and Applications*; Springer Science & Business Media: Berlin/Heidelberg, Germany, 2011.
44. Gonçalves, T.; Silva, R.; de Brito, J.; Fernández, J.; Esquinas, A. Mechanical and durability performance of mortars with fine recycled concrete aggregates and reactive magnesium oxide as partial cement replacement. *Cem. Concr. Compos.* **2020**, *105*, 103420. [CrossRef]
45. Vandeperre, L.; Liska, M.; Al-Tabbaa, A. Microstructures of reactive magnesia cement blends. *Cem. Concr. Compos.* **2008**, *30*, 706–714. [CrossRef]
46. Jang, J.-K.; Kim, H.-G.; Kim, J.-H.; Ryou, J.-S. The evaluation of damage effects on MgO added concrete with slag cement exposed to calcium chloride deicing salt. *Materials* **2018**, *11*, 793. [CrossRef] [PubMed]
47. Zhang, R.; Panesar, D.K. Mechanical properties and rapid chloride permeability of carbonated concrete containing reactive MgO. *Constr. Build. Mater.* **2018**, *172*, 77–85. [CrossRef]
48. Meddah, M.S.; Suzuki, M.; Sato, R. Influence of a combination of expansive and shrinkage-reducing admixture on autogenous deformation and self-stress of silica fume high-performance concrete. *Constr. Build. Mater.* **2011**, *25*, 239–250. [CrossRef]
49. EN 1992-1-1:2004/A1:2014. *Eurocode 2: Design of Concrete Structures-part 1-1: General Rules and Rules for Buildings*; European Committee for Standardization: Brussels, Belgium, 2004.
50. Wittmann, F. Crack formation and fracture energy of normal and high strength concrete. *Sadhana* **2002**, *27*, 413–423. [CrossRef]
51. Li, Y.; Deng, M.; Mo, L.; Tang, M. Mechanical properties of concrete with light burnt MgO-based expansive additive under different restrained conditions. *J. Cent. South Univ. (Sci. Technol.)* **2012**, *43*, 2534–2541.
52. Müller, H.S.; Breiner, R.; Anders, I.; Mechtcherine, V.; Curbach, M.; Speck, K.; Dehn, F.; Walraven, J.; Reinhardt, H.-W.; Lohaus, L.; et al. *Code-Type Models for Structural Behaviour of Concrete: Background of the Constitutive Relations and Material Models in the Fib Model Code for Concrete Structures 2010*; State-of-Art Report Internat; Federation for Structural Concrete: Lausanne, Switzerland, 2010; 196p.